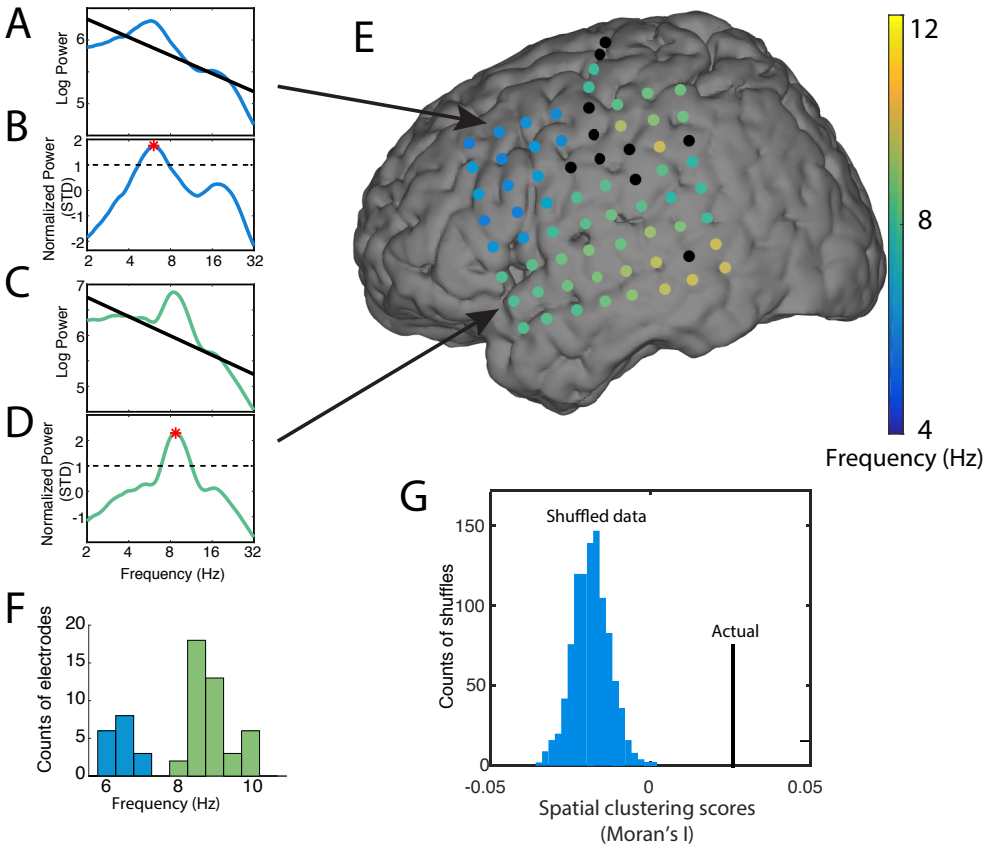

Supplemental Figure S1: **Oscillation clusters across neocortical space. Related to Figure 1.** (A) Power spectra at an example electrode in Patient 77. Blue line shows the mean power spectrum; the black line indicates the background $1/f$ signal estimated with a robust fit regression (Manning et al., 2009). (B) Normalized power spectrum, computed as the difference between the raw power spectrum and the $1/f$ background signal from Panel A. The dotted line shows the threshold for detecting true narrowband oscillations; red asterisk shows the local maximum above this threshold, thus revealing a narrowband oscillation at 6.1 Hz. (C & D) A different electrode in this patient with a narrowband oscillation at 8.8 Hz. (E) All electrodes in this patient, colored according to the frequency of the narrowband oscillation at each site. Black indicates electrodes without narrowband oscillations. (F) Histogram of the frequencies of the oscillations across this grid. Blue and green colors indicate electrodes in the 6.1- and 8.8-Hz clusters, respectively. (G) Analysis of the spatial clustering of oscillation frequencies across all patients. Black line indicates the mean Moran's I statistic (Moran, 1950). The mean I is positive and outside the distribution of statistic values estimated from shuffling (blue bars), which indicates that oscillation clusters are reliably clustered spatially ($p \ll 10^{-3}$, permutation test).

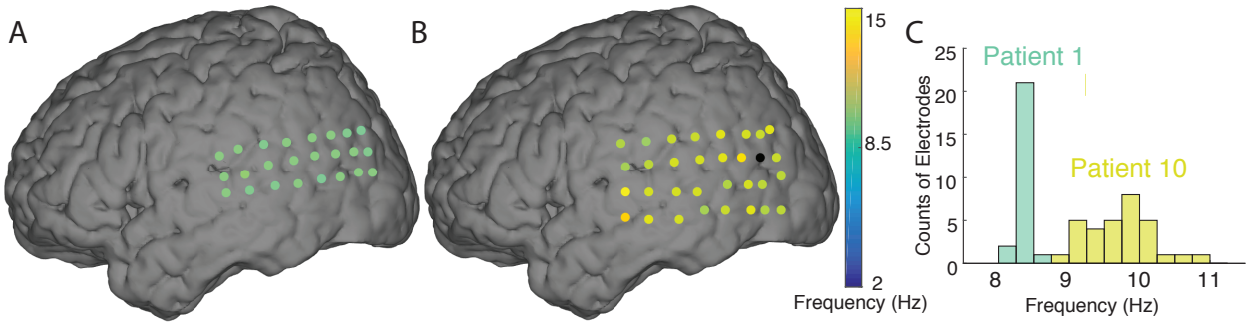

Supplemental Figure S2: **Interindividual differences in oscillatory frequency. Related to Figure 1.** (A & B) Brain plots indicate the frequencies of oscillations observed at individual electrodes in Patients 1 and 10, respectively. (C) Distribution of narrowband oscillation frequencies across electrodes. The frequencies between these patients are nonoverlapping, which indicates that each subject has distinctive frequencies even though the electrodes sample similar regions.

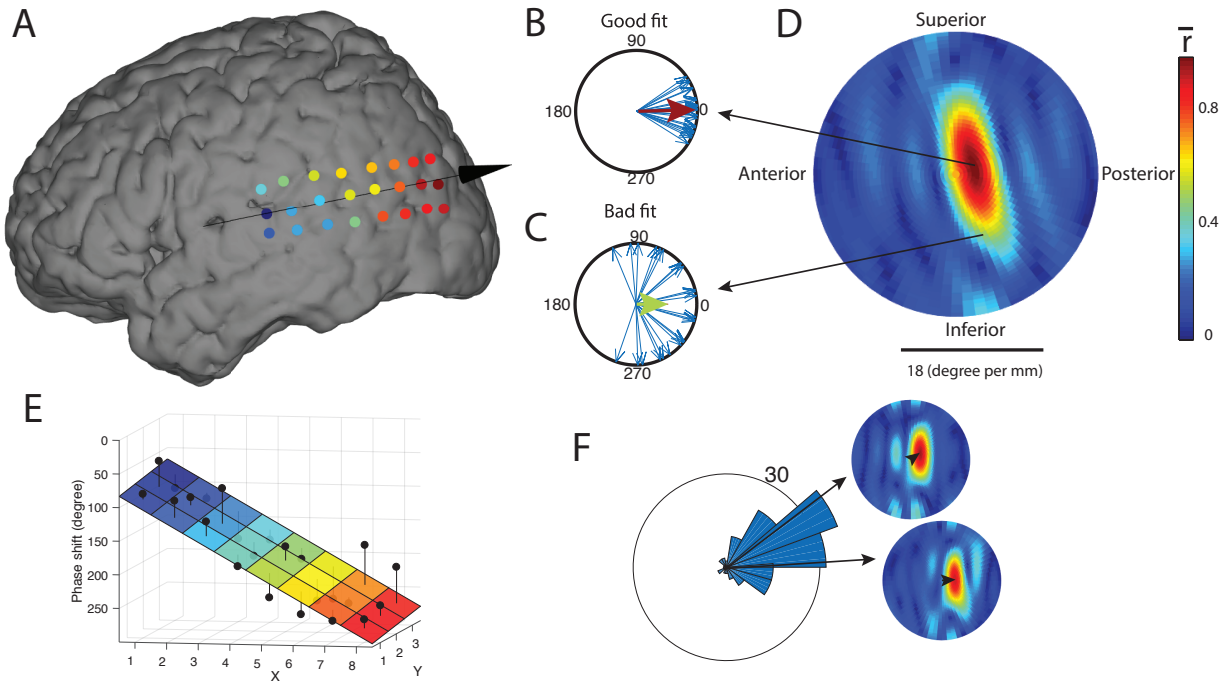

Supplemental Figure S3: **Methodology for characterizing the propagation of individual traveling waves. Related to Figure 1.** (A) Spatial distribution of oscillatory phase for a traveling wave in Patient 1 on one trial. (B) Residuals of best fitting circular–linear model for this trial. Each blue arrow indicates the residual from one electrode; red arrow is the mean resultant vector of all residuals ($\bar{r} = 0.98$). (C) Residuals from a suboptimal set of model parameters, shown for illustrative purposes. The length of the resultant vector from this model ($\bar{r} = 0.5$) is shorter than the model from Panel B. (D) Fits for all possible circular–linear models for this trial. The color surface indicates the fitted model $\bar{r}$ for all possible propagation directions and speeds. (E) Visualization of the fitted model from Panel B. Color indicates the plane of phase predictions; black dots indicate the observed phases; black lines indicate residuals. (F) Histogram of propagation direction across all trials for this cluster, calculated based on the best fitting model from each individual trial on this cluster. Inset plots show the full distribution of circular–linear model fits for two additional selected trials.

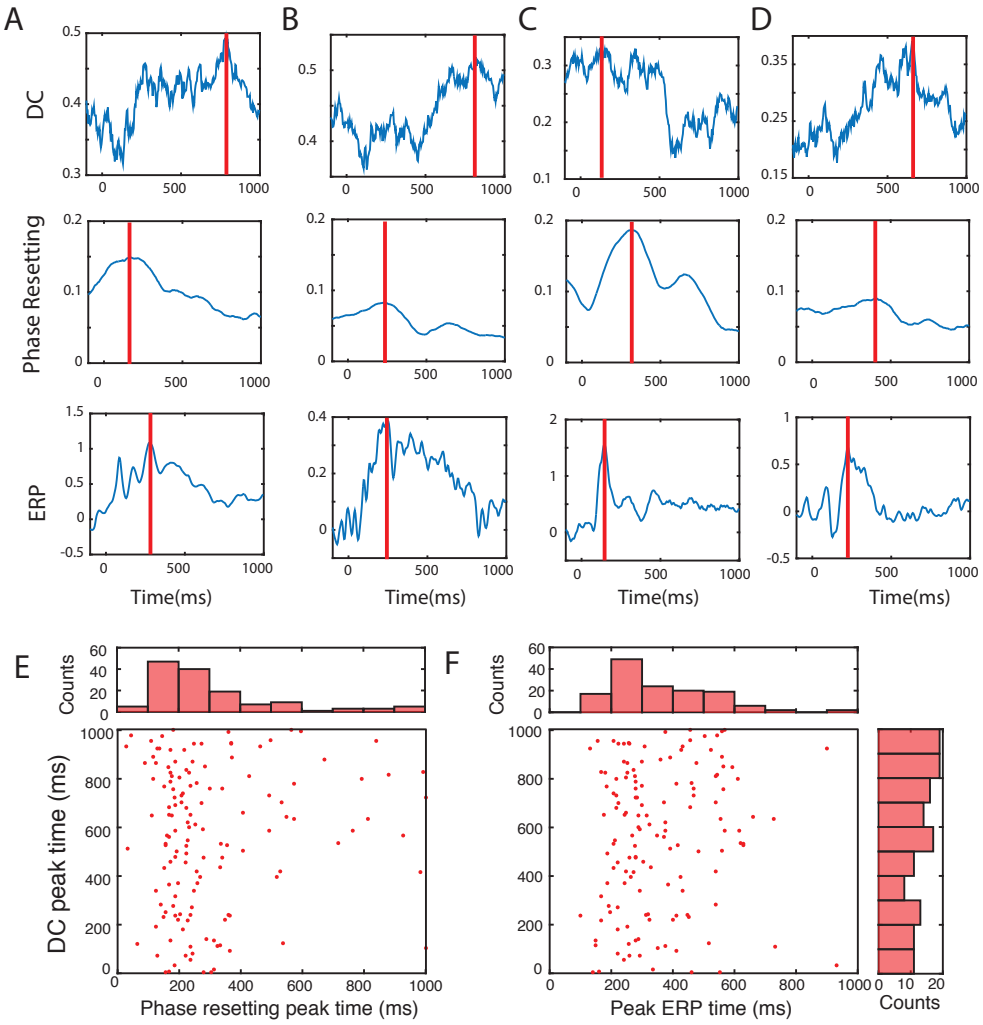

Supplemental Figure S4: **Relation between traveling waves and evoked signals. Related to Figure 4.** (A) First row, timecourse of traveling wave directional consistency (DC) for the same oscillation cluster as in Fig. 1A–G. Red line shows timepoint of peak value. Second row, timecourse of mean phase resetting score ($\bar{r}$) across all electrodes in this cluster at the traveling wave's temporal frequency. Third row, event related potential (ERP) from an electrode in this cluster. (B) Same information as in Panel A, but for the cluster of electrodes shown in Fig. 1H. (C) Same information, but for the cluster of electrodes shown in Fig. 4C & D. (D) Same information , but for the cluster of electrodes shown in Fig. 1I. (E) The relation between the timepoints of peak traveling wave DC and of peak phase resetting. Each point indicates these two values for a single cluster that showed a traveling wave. There was no significant correlation between these distributions ($r = 0.08$, $p > 0.1$). (F) The relation between the timepoint of peak traveling wave DC and the timepoint of the largest ERP modulation for that cluster—there was no significant correlation ($r = 0.02$, $p > 0.1$).

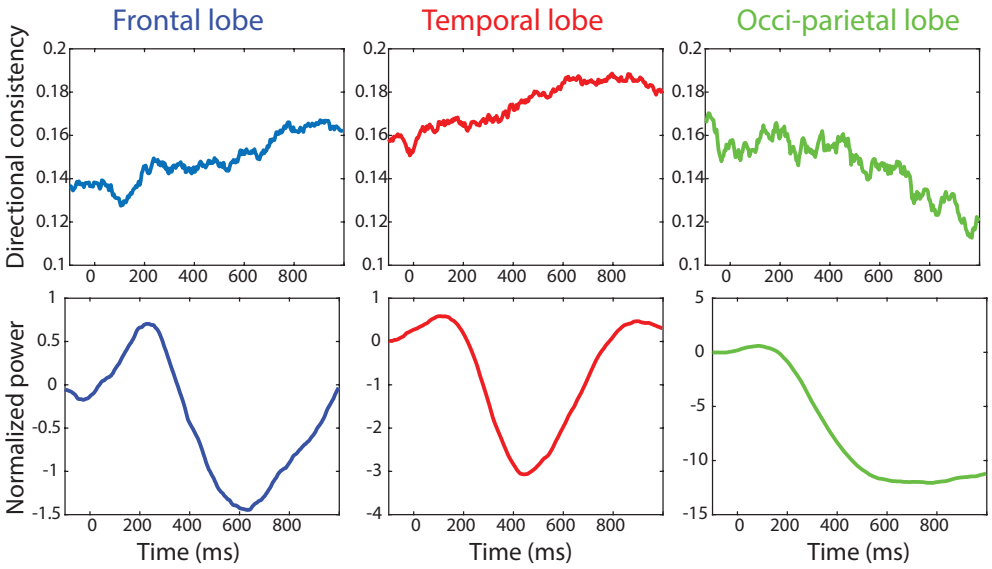

Supplemental Figure S5: **Relation between traveling wave DC and Oscillation power. Related to Figure 4.** First row, the mean DC course of the traveling waves across different regions (replicated from Fig. 4E). Second row, the average power of traveling wave clusters across different regions. Power was measured at the individual frequency of each traveling wave cluster.

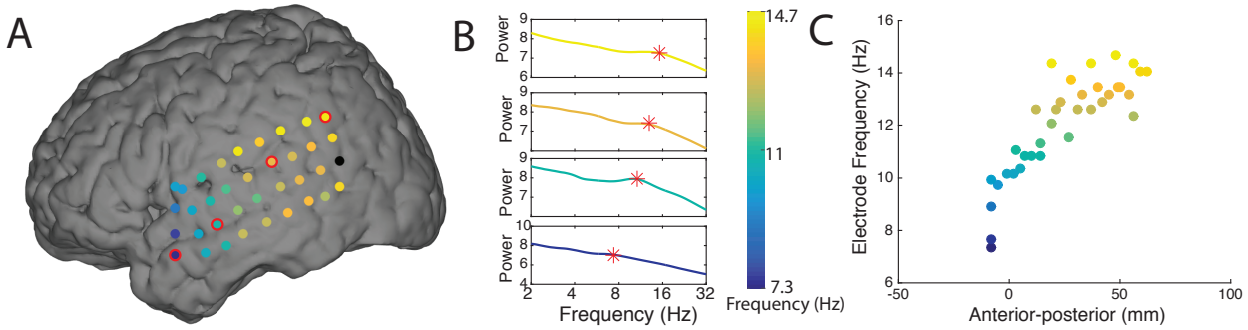

Supplemental Figure S6: **Example oscillation frequency gradient. Related to Figure 7.** (A) Brain plot of the frequencies of oscillations in Patient 18. (B) Power spectra from four selected electrodes, which correspond to the sites labeled with red circles in Panel A. Red asterisks indicate the identified peak narrowband oscillation frequency on each spectrum. (C) Scatter plot showing the relation between each electrode's oscillation frequency and its location along the anterior–posterior axis.

Patient number	Electrode coverage: Left hemisphere	Electrode coverage: Right hemisphere	Sex	Age	Handedness	Traveling waves
1	TO grid					LTα
2	strips		M	17	Right	LTθ LFθ
3	F Grid + midline Grid + strips		M	15	Right	LFθ LFθ
4	strips	T grid+ strips	F	8	Right	
5	P Grid + strips	strips	M	17		
6		T grid + strips				RTθ RTθ RPα RTα
7	F grid +strips	strips	F	20	Right	RFθ LFθ RFθ
8		strips				
9		POT grid				RPθ
10	TO grid					LPα
11	PT grid	strips				RTθ LPα
12		P strips				RPθ
13		TPO grid	M	20	Right	RPθ
14	strips		F	53		
15	T grid		M	50	Right	LPθ LTα
16	F grid + TO grid		M	28		LTα
17	strips		F	30		
18	T grid		M	23		LTα
19	T grid	strips	M	18	Right	LTθ LTθ LTα
20		strips	F	43		RTα
21		strips	M	42		RTθ RTα
22	strips		F	22	Left	LTθ
23		T grid + strips	M	47	Right	RTα RTα
24	strips	strips	F	27	Right	RTθ
25		strips	M	20	Right	RFθ
26	FP grid +strips		M	16	Right	LFθ LFα
27		T grid	M	15	Right	
28	TPO grid		M	21	Right	LTθ LTα LTα
29	strips	strips	F	40	Right	LTθ RTα LTα
30	strips	strips	F	34	Right	RTα LTα
31	strips	strips	F	34	Right	RTα RFθ LTα
32	strips	F grid + P grid + T grid	F	39	Right	RPα RTα RFθ
33		FP grid + strips	M	30	Left	RFθ RFθ RPθ RFα RFα
34	F_θP grid + strips	strips	F	23	Right	LTα
35	strips		M	29		LFα LTα
36	FP grid + strips		F	25	Right	
37	strips	strips	M	43	Right	
38	strips		F	38	Left	LTα LPα
39	TP grid + strips	strips	M	21	Right	LFθ LFθ LFθ LTα RFα
40	strips		M	56	Right	LTθ
41	TP grid + strips		F	57	Right	LTα
42	strips	strips	M	20	Right	LFθ RFθ
43	strips	strips	M	20	Right	RFθ LFθ RFθ LFθ
44		strips	M	41	Right	RTα RPα
45	T grid + strips		F	34	Right	RPα
46		TP grid +strips	F	52	Left	RTα
47	strips	strips	M	44	Right	RFθ RTα
48	strips	strips	M	35	Right	RFθ RFθ RPθ LFθ
49	strips	strips	F	44	Right	LTα RTα
50	strips	strips	M	33	Right	RFθ LFθ RTα RPα LTα
51	strips	TO grid + strips	F	23	Right	
52	strips	strips	F	48	Right	LTα
53	strips	strips	M	45	Right	RTα RTα LTα
54		strips	M	15	Right	RTθ
55	strips	strips	M	53	Right	LTθ
56	strips	strips	M	29	Right	LFθ LTα
57	strips	strips	F	48	Right	RPα LPα
58	strips	strips	F	20	Right	RFθ RFθ RFα RFα LPα
59	strips	strips	M	50	Right	LFθ LFα
60	strips	strips	M	18	Right	LTα
61	strips	strips	F	44	Right	LTθ LFθ RTα LTα
62	strips	strips	M	28	Right	LFθ
63	strips	strips	F	26	Right	RFα LFθ
64	strips	strips	F	27	Right	LTθ
65	strips	strips	F	55	Left	LFα RFα RPα
66	strips	TPO grid+ strips	F	58	Right	RTα
67	strips	strips	M	18	Ambidextrous	
68	FP grid +strips	strips	F	49	Left	LFθ LFθ LPθ
69	strips	strips	M	40	Right	LPα RFθ RTθ
70	strips	strips	M	37	Right	LFθ RFθ
71	FP grid +strips	strips	M	20	Left	LFθ RFθ LFα
72		FTP grid+ strips	M	37	Right	RFα
73		T grid	M	42	Right	
74	strips	FTP grid+ strips	F	28	Left	RFθ RFθ
75	strips	strips	F	30	Left	LFθ LFθ LFθ RTθ RPθ
76	FTP grid + strips		M	33	Right	
77	FTP grid + strips		M	37	Right	LTα

Supplemental Table S1: **Summary of complete dataset. Related to Figure 3.** Each row summarizes the clinical electrode positioning in one patient. Region Key: F, Frontal; T, temporal; O, occipital; P, parietal. The column labeled "Traveling waves" describes the properties of any oscillation cluster with significant traveling waves. Greek letters indicate its frequency band (θ, 2–8 Hz; α, 8–15 Hz).

	Left frontal	Right frontal	Left temporal	Right temporal	Left parietal	Right parietal	Left occipital	Right occipital	Total
No oscillation	125	158	85	148	48	47	2	14	627
Non clustered oscillation	193	172	212	219	90	87	18	58	1049
Clustered non-TW	34	138	139	88	34	52	10	10	505
Traveling Waves	579	278	352	329	134	160	29	35	1896
Total	931	746	788	784	306	346	59	117	4077

Supplemental Table S2: **Counts of electrodes with different oscillatory properties across regions. Related to Figure 3.** Columns denote brain regions and rows correspond to oscillatory properties (see *Methods*). *No oscillation* denotes electrodes that showed no narrowband oscillations. *Non clustered oscillation* indicates of electrodes that showed narrowband oscillations but were not part of an oscillation cluster. *Clustered non-TW* denotes electrodes that were a part of an oscillation cluster but did not demonstrate a traveling wave according to our criteria. *Traveling waves* denotes the counts of electrodes that showed robust traveling waves.

Traveling wave feature	Mean for fast response	Mean for slow response	Relative change	T stat	P value
PGD	0.47	0.47	0.93%	t_{139}=2.99	0.003
DC	0.18	0.16	11.9%	t_{139}=5.56	10^{-7}
Power	1.28	1.27	1.04%	t_{139}=4.11	10^{-5}
Temporal frequency (Hz)	7.42	7.44	-0.16%	t_{139}=-0.22	0.82
Spatial wavelength (m)	0.11	0.11	0.62%	t_{118}=0.63	0.52
Propagation speed (m/s)	0.54	0.54	0.07%	t_{118}=0.05	0.96

Supplemental Table S3: **The relation with behavior for different features of traveling waves. Related to Figure 5.** Columns 2 & 3 provide the mean value of each traveling-wave feature (see *Methods*) on trials where patients responded with fast (good) and bad (slow) response times, as identified with a median split. Statistical significance is assessed with a paired t test.